

Detecting plant seasonality from webcams using Bayesian multiple change point analysis

5 Raimund Henneken ¹, Volker Dose ², Christoph Schleip ¹, Annette Menzel ¹

Addresses:

¹ Fachgebiet für Ökoklimatologie, Technische Universität München

10 Hans-Carl-von-Carlowitz-Platz 2, 85354 Freising

² Max-Planck-Institut für Plasmaphysik (IPP),

Boltzmannstrasse 2, 85748 Garching

15 **Correspondence author:**

Raimund Henneken, henneken@wzw.tum.de, fax: 0049-8161-714753

Running title (less than 45 characters):

20 Bayesian analysis of seasonal change points

Total amount of words :

6.674

Summary (344 words)

1. Phenological observations have a long tradition. By contrast, digital webcam-based phenological research has only developed in recent years, prompted by the development of cheaper user-friendly digital camera systems and by higher staff costs. Webcam photography provides spectral information in red, green and blue (RGB) wavelengths which mirror the seasonal colour changes in trees during bud burst, leaf unfolding, senescence and leaf fall.
2. Recent publications have mainly used two types of image data analysis to define onset dates of certain phenological stages and to compare species and growing seasons. These methods work well, but require high quality of the webcam images. However, changing light and weather conditions complicate data analysis at increasing camera-to-subject distances. We investigated a series of images providing colour information on different tree species, e.g. *Fagus sylvatica*, *Populus tremula*, as well as of trees at different altitudes (700-1200 m) in the Bavarian Forest National Park, Germany. Webcam images were analysed by the two previously published methods and compared with results derived from a newly developed Bayesian multiple change point analysis.
3. The Bayesian analysis described phenological transition dates in spring and autumn accurately and specified the uncertainties of the model fit. By contrast, the compared methods revealed weaknesses regarding the quality and consistency in identifying phenological transitions.
4. Deciduous autumn phenology was detected similarly accurately by change point models. In particular, transition dates of leaf development were identified in the green, as well as the red, colour channel.

5. The change point analysis at different elevations showed how the Bayesian approach coped with continuously degrading image quality. A delay in green-up of about 2.5 days per 100 m of altitude was estimated for *Fagus sylvatica* in the study area. Autumn phenology in different altitudes did not show clear patterns.
6. The Bayesian model approach allows not only the calculation of phenological change points during the year but also estimates the probability of changes occurring on a particular day. This method leads to a higher accuracy in estimating phenological events in the growing season, especially when handling low quality webcam data.

Key-words

altitudinal gradient, Bayesian statistics, digital photography, spring green-up, leaf colouring, leaf fall, multiple change point model, phenology, webcam

Introduction

Phenology is “probably as old as civilization itself” (Schwartz 2003). Almost certainly, early Man was aware of the relationship between plants and their environment in order to help with the cultivation of crops, or the exploitation of wild resources.

Phenological observations have a long history. Started with first phenological calendars recorded by the Ancient Greeks phenology developed to one of the main research fields for assessing the impact of climate change on ecosystems (Menzel 2002). Sparks *et al.* (2009) showed the growing importance of phenological research from 1990 to 2009 which can be linked to increasing air temperatures and the demand for indicators of the influence of climate change on the biosphere. In recent years, various studies have focussed on the effect of global warming on phenology (Menzel *et al.* 2006, Rosenzweig *et al.* 2008, Jeong *et al.* 2011).

Menzel (2002) suggested that phenology is probably the easiest way to track climate change effects on species, however it is both labour- and time-intensive, therefore satellite- or webcam-based observation methods have been investigated as possible alternatives. Due to the insufficient spatial and temporal resolution of satellite recordings, inexpensive automated digital cameras have increasingly become popular alternatives to the current system of phenological monitoring of ecosystems (Richardson *et al.* 2007, Ahrends *et al.* 2009, Richardson *et al.* 2009, Ide & Oguma 2010, Kurc & Benton 2010, Nagai *et al.* 2011). Furthermore, analyses of worldwide, and freely available, outdoor webcam images have proved to be a useful alternative to both ground and satellite phenological observation methods (Jacobs *et al.* 2009; Graham *et al.* 2010).

Digital cameras store spectral information in red, green and blue colour channels. Changes which occur in this colour information during the year can be directly linked to phenological changes. Estimating spring green-up from the green colour channel (Ahrends *et al.* 2009, Richardson *et al.* 2009, Ide & Oguma 2010) as well
5 as detecting leaf colouring in autumn from red colour channel information (Richardson *et al.* 2009) has been achieved. However, these analysis methods, when applied to other species and/or locations, have not shown the same suitability as in the original publications.

Dose & Menzel (2004) introduced Bayesian analysis for the detection of a change
10 point in phenological time series. That study as well as those of Schleip *et al.* (2006) and Menzel *et al.* (2008) demonstrated the possibilities of Bayesian statistics for analysing functional behaviour in ecosystems.

In the current study, we applied Bayesian analysis to describe phenological events such as leaf unfolding and maturity in spring, and leaf colouring and fall in
15 autumn. Therefore a multiple change point analysis based on the Bayesian one change point model (Dose & Menzel 2004) was developed. In addition to a phenological analysis of deciduous tree species at an altitudinal gradient in the Bavarian Forest National Park in Germany we highlighted differences between recent image data analysis methods and our Bayesian multiple change point
20 method.

Materials and methods

STUDY SITE AND CAMERA SETUP

The mountain “Grosser Falkenstein” (49°05’N, 13°16’E; 1315 m a.s.l.) is located in the Bavarian Forest National Park in the south-east of Germany, 3 km west of the Czech border. The mountain rises some 600 m above its surroundings. The climate is humid continental, the mean annual temperature varies between 3 and 5 °C and the annual precipitation is about 1400 mm, of which a third derives from fog. At higher elevations, snow cover lasts up to 8 months (German Meteorological Service, National Park Administration).

A digital single-lens reflex camera (Canon EOS 350 D) facing slightly upwards to the south slope of the mountain was installed on an outside wall of a house. Between March 2006 and August 2007 the camera was automatically controlled by a timer and took daily JPEG images (image resolution of 7.9 MP) in the early afternoon (1-3 h p.m.). Exposure and aperture mode, as well as the white balance, were set to automatic.

The images displayed about 600 metres altitudinal difference. Trees in the foreground were located within 50 to 350 m of the camera at the edge of a settlement (Lindberg, 680 m) (Fig. 1). These species were European Silver Fir, *Abies alba* MILL., Norway Spruce, *Picea abies* (L.) H. KARST., Common Beech, *Fagus sylvatica* L. and Common Aspen, *Populus tremula* L.. Remote trees on the slope in the background were at a distance of 2.5 to 5 km from the camera and mainly consisted of Norway Spruce and Common Beech; sporadically European Larch, *Larix decidua* MILL. occurred in small groups at 800-1000 m.

DATA PROCESSING

Contour lines were created and afterwards distorted to the camera's perspective using ESRI ArcScene (3D visualization application for GIS data), an elevation model and the relevant geo-coordinates (camera site, mountain peak). In a second
5 step, the contour lines were transferred onto an image by using picture processing software (Adobe Photoshop) and then indicated the altitudinal bands for further analysis.

Because the camera was installed for educational, and not for scientific purposes, just one image was taken per day. By contrast to the image quality control
10 measures of Ahrends *et al.* (2009), who excluded images from days with critical light or weather conditions such as rain, fog and snow, we analysed the entire raw data set.

Image analysis was conducted by defining different regions of interest (ROI) as described by Richardson *et al.* (2007), Richardson *et al.* (2009) and
15 Ahrends *et al.* (2009). For each ROI a mask (binary image) was created. Three ROI of foreground trees (hereafter called beech, aspen1 and aspen2) were selected manually based on various images as a compromise between maximizing the size of the ROI and avoiding disturbances in the background from tree species with different phenological behaviour (Fig. 1).

20 For the analysis of altitudinal bands, the use of non-rectangular and discontinuous ROI was necessary to separate Common Beech (deciduous) and Norway Spruce (evergreen) trees during the data processing. For creating masks of the altitudinal ROI which covered Common Beech trees, image sections with similar colour values were tagged using the "Magic Stick" tool (Adobe Photoshop, tolerance
25 value 8) using an image from May 22 2006 (day of year (DOY) 142, Fig. 1).

Similarly to the methods of Richardson *et al.* (2007), a custom script (Python Software Foundation) colour-split the digital image files sequentially and, taking the mask into account, extracted and averaged the colour channel information (digital numbers; red DN, green DN, blue DN). This procedure was repeated for
5 each mask/ROI. The overall brightness of each ROI (eqn 1, DN = digital number) and the proportional value for the green and red colour channels (eqn 2) were calculated to minimize the influence of sunshine differences between days.

eqn 1 **total RGB DN = red DN + green DN + blue DN**

10 eqn 2 **green% = green DN / total RGB DN**

red% = red DN / total RGB DN

DETECTING SEASONALITY BY FORMERLY APPLIED METHODS

For detecting different phenological stages in the seasonal development of
15 deciduous trees, we used the two methods proposed by Richardson *et al.* (2007, 2009) as well as Ahrends *et al.* (2009).

Following Richardson *et al.* (2007, 2009), we fitted sigmoid-shaped logistic functions to the green% and red% time series (eqn 3 and eqn 4, respectively). The parameters a and b define the lower (a) and upper (a + b) limits of the function.
20 For eqn 3, the parameter c controls the position, d the overall steepness of the function, or rather of the spring green-up and the autumn photosynthetic degradation.

eqn 3 **$f(x) = a + b / (1 + e^{(c-d*x)})$**

25

The day of year at which $f(x) = a + (b/2)$, thus the functions achieve its half-maximum (hereafter hspring and hautumn) represent a benchmark to compare

patterns between growing seasons and the phenological behaviour of different species.

eqn 4
$$f(x) = a + b / ((1 + e^{(c-d*x)}) * (1 + e^{(e-f*x)}))$$

5

Since the red colour values show an increase and subsequent decrease during autumn, the expanded logistic function (eqn 4) was applied to fit the red% time series. In this case, parameters c and d control the position and steepness of the increase of red% during leaf colouring, e and f the decrease of red% during leaf fall. For comparisons, the day at which the fit achieves its maximum was calculated (hereafter xautumn).

A different approach to characterize the annual phenology of various tree species was provided by Ahrends *et al.* (2009). In an analogous manner, relative colour information was extracted from webcam images. Using a methodology adapted from Zhang *et al.* (2003), transition dates were derived from time series as follows:

(1) the start of the growing season (SOS) – date of budburst of deciduous trees or start of photosynthetic activity in general; (2) start of leaf senescence (SEN) – decreasing of photosynthetic activity, deciduous tree leaves become coloured; (3) end of growing season (EOS) – end of physiological activity, complete foliage loss. Zhang *et al.* (2003) mentioned a fourth transition date: “maturity – the date at which plant green leaf area is maximum” which was also included in the data analysis by Ahrends *et al.* (2009). The so called “GF_{max}” (hereafter MAT) describes the leaf maturity, the date when leaves had completely unfolded.

MAT was defined as the date with the highest green% value. SOS, SEN and EOS were determined by using piecewise first and second derivative analyses.

Piecewise derivatives involve calculating the slope at day x from values at days $x-1$ and $x+1$ (eqn 5).

eqn 5 **slope (x) = (y_{x+1} - y_{x-1}) / 2**

5

Derivatives were calculated and smoothed by 11 point moving averages, start and end sections derived from fewer values were excluded from further analysis. SOS was identified as the maximum of the smoothed second derivative. Counting backwards from the minimum of the smoothed first derivative (negative value), SEN was estimated as the day when the first value became positive. Starting from the minimum value, working forwards, the end of the growing season (EOS) was estimated when the first derivative became positive.

10

In addition to these transition dates we also intended to estimate the day at which the colouring process was completed and defoliation started (SOF – start of leaf fall). In high quality webcam datasets of deciduous tree phenology, green channel values increase again after being reduced during leaf colouring, at SOF red channel values decrease after reaching their maximum.

15

DETECTING SEASONALITY BY MULTIPLE CHANGE POINT ANALYSIS

20

The present study is an extension of the Bayesian one-change-point model presented by Dose & Menzel (2004) for the analysis of phenological time series. This earlier work employed a function consisting of two straight line segments joining at the change point t_c that can be at any time after the beginning of the time series t_i ($t_i < t_c$) and before the end of the series t_e ($t_c < t_e$).

25

While traditional least squares methods would determine t_c as the time t_{ML} yielding the best fit to the data and consequently result in triangular functions, the

Bayesian approach also considers change points in the neighbourhood of the maximum likelihood change point. The calculation of the probability of the change point position shows that a number of choices around the maximum likelihood value have comparable probability to t_{ML} . The Bayesian answer to the fit problem is therefore a superposition of all triangles weighted by their respective probabilities. The resulting function may not at all resemble a triangle.

The extension of this one-change-point model consists of a polygon with more than two linear sections. For n sections there are then $n-1$ change points where the linear segments match to ensure continuity. With n datapoints we have $n-2$ choices for the first change point, $n-3$ for the second etc. A two change point model offers nearly $(n-3)^2$ different possibilities for the two positions. The computational effort rises dramatically with an increase in the number of change points.

Within Bayesian probability theory it is possible to calculate the probability of the number of change points. This probability passes through a maximum characterized by the tradeoff between better fit with increasing number of change points and the concomitant increasing complexity of the data description. The mechanism is called Ockham's razor (Garret 1991). In fact, $n-2$ change points would provide an alternative exact description of the data and nothing would be gained from the analysis. Progress in understanding is achieved from a parsimonious description of the data which captures the essentials and reduces the noise.

Fig. 2 shows an example of the fit of a two change point function to a time series with data shown as open circles. Two change points had the overwhelming probability in this case. The Bayesian analysis does not only allow for an estimate of the fit function but also for the associated uncertainty. The uncertainty is shown

as a shaded band in Fig. 2. Note the slight increase in the uncertainty at the ends of the time series and near the change points. In these regions the function estimate is based on a reduced number of data. The lower panel of Fig. 2 shows the calculated normalized change point probability distributions.

5 In this paper we present the results of the Bayesian analysis of the National Park datasets. However, rather than display results like in Fig. 2, we summarize the change point probability distributions by their means and standard deviations and the quality of the fit by the root mean square deviation.

There is, of course, some mathematics behind this description of the multiple
10 change point problem. Those interested in these technical details are referred to the supporting information of this paper.

Results

From the raw data two sets characteristic for spring and autumn phenological behaviour were deduced. The spring data range from DOY 80 to DOY 170. For autumn DOY 200 to day 35 of the following year, hereafter denoted DOY 400 were chosen. For both types of datasets buffer times of at least twenty days before and after an expected transition were included. All datasets were analysed with functions containing 1 to 8 change points. The prominent result of this analysis is the probability of the respective change point functions. The following results, however, refer always to the model with the highest probability.

10

Comparison of methods

The best change point models (further called CPM) for green% spring time series 2006 and 2007 were those with two change points. Fig. 3 summarises the CPM of aspen1 including the results from the two established methods, Table 1 displays further results for all foreground region of interests.

In both years the CPM of aspen1 gave a reasonable fit of the green% time series. Data for 2007 were more variable than in 2006 which is mirrored in a wider deviation band of the CPM and of the mean of the change point probability. Both CPM feature a slight and steady increase of green% before green-up (SOS) and decrease after MAT. This behaviour can not, by definition, be described from the logistic function leading to an unreasonable fit and estimating the hspring date too early.

Comparing to the CPM, SOS transition dates of aspen1 were estimated 2 days earlier in 2006 and 2007 by the method of Ahrends *et al.* (2009). MAT dates, described by the maximum green% value, were approximately 13 and 2 days later, in 2006 and 2007 respectively, than those from the CPM.

Beech spring phenology shows a similar pattern to aspen1 (Table 1). SOS and MAT occur earlier in 2007 than in 2006, however, leaf development took 2 days longer than in 2006. Ahrends *et al.* (2009)'s SOS dates were nearly the same as from the CPM, MAT dates were estimated later. For aspen2, leaf up had a duration of 27 days in 2006, but only 6 days in 2007. The compared methods showed less difference in the duration of green-up, 18, respectively 13 days.

In autumn, only data from year 2006 were available. The results of the autumn CPM were variable regarding the number of change points in the best model fit. Three transition dates were expected in both green% and red% time series, i.e. SEN, SOF and EOS. However, the calculated number of change points differed between 1 and 4, which affects the evaluation of the CPM (Table 2).

In general, change points were assigned to phenological transitions by visual assessment. In the case of just one change point (red% of aspen1), the change point matched the maximum red value, thus, it was associated with SOF. In the case of two calculated change points (green% of aspen1), the first change point may represent SEN, the second seems to be located between SOF and EOS. In the case of four change points, one change point more than expected was revealed by the Bayesian analysis. These additional change points did not affect the determination of the seasonal transition days.

Fig. 4 shows CPM for green% and red% of aspen2 in autumn 2006. In both CPM at least 3 change points were estimated by the Bayesian analysis, green% time series was best described with an additional fourth change point in the decreasing leaf green part after SEN. In general, green% and red% transition days matched each other and did not differ by more than 2 days (Table 2). The green% CPM estimated a 11-day period of leaf senescence (SEN till SOF) instead of 14 days by

red%. Defoliation (SOF till EOS) took 4 days assessed in green% instead of 5 days in the red% time series.

As described above, the green% and red% logistic fit can not accommodate increases before and decreases after transition dates. By definition, changes in the green channel after leaf fall (from SOF on) cannot be detected either. In the red channel of aspen2 the maximum of the logistic fit (xautumn) estimated SOF 2 days earlier than from the CPM. Transition dates derived from derivatives (Ahrends *et al.* 2009) indicated a much earlier SEN at DOY 275, and EOS date (DOY 304) just one day earlier compared with the CPM.

Autumn analysis of the beech ROI showed a similar phenology to aspen2, although transition days SOF and SEN in both colour channels differed up to 6 days. The standard deviation of SEN of red% is very large, which is not apparent in the green% time series. Due to fewer estimated change points of aspen1 a comparison with other ROIs is difficult. The CPM describes the green% SEN just one day before red% SOF, which has a higher uncertainty (SD = 5.9 days), EOS of green% is estimated 4 days later than red% SOF at DOY 309.

ALTITUDINAL STUDY

Results of the CPM of altitudinal bands in spring 2006 are displayed in Fig. 5.

Except for the 800-900 m band, the best CPM were based on two change points. The third change point at 800-900 m interrupted the decreasing post-MAT part of the time series by a further increase. This behaviour may also be apparent for the 900-1000 m band, though the CPM selected two change points instead. In 2006, SOS and MAT became later with increasing altitude, SOS changing from DOY 120 to 130, MAT from 129 to 137 (Table 3). There was no clear pattern between altitude and the length of leaf development, i.e. in MAT-SOS. Standard

deviations of change points increased with higher altitude, most likely due to decreasing image quality.

Two remarkable days with exceptional high green% values appeared in every altitudinal band, at DOY 139 and 142. Due to good visibility DOY 142 had
5 maximum green% values, which would cause Ahrends *et al.* (2009)'s method to define it as MAT. By contrast, the CPM reveal more reasonable earlier MAT dates.

The altitudinal analyses of green% time series in 2007 showed an earlier green-up than in 2006, although leaf development might have been longer at higher
10 locations. In comparison to 2006 the standard deviation of the transition dates did not increase with altitude.

For the autumn phenology in altitudinal bands the Bayesian analysis revealed that the CPM of red% were based on one change point, green% data on two or three change points (Table 4). Dates for SEN, SOF and EOS based on green% seem
15 reasonable in their timing. However, red% time series were characterised by extremely high standard deviations and seem less suitable. Thus the fact that SOF of red% occurs after EOS of green% and that the general timing is in fact too late in the season should not be over interpreted.

Results based on CPM did not show a clear pattern between altitude and autumn
20 phenology. For example, SEN was earlier from 700 m to 1000 m on, but reversed above this height, the altitudinal pattern for green% EOS was also ambiguous.

Discussion

The phenological responses of tree species differ greatly (Menzel 2003). Timing of bud burst, the duration of leaving, leaf colouring and fall are optimised for survival and reproduction strategies. However, phenological phases are greatly
5 affected by variation in weather which strongly impacts on the development of the annual lifecycle. Therefore an evaluation method of phenological time series, also from digital cameras, must operate adequately across a range of species and environments.

Our study gives an overview of recent methods and introduces the Bayesian
10 multiple change point method in the analysis of phenological transition dates. The phenology of beech and aspen from distances closer to the camera indicated the potential for comparing growing seasons since the CPM described the green% time series with high accuracy and detected expected change points with low uncertainty (Fig. 3).

15 Differences between 2006 and 2007 in the timing and the duration of green-up reflected differences in spring temperatures. March and April mean temperatures in 2006 were about 5 °C lower, and May mean temperature about 1.7 °C lower, than in 2007 (German Meteorological Service, station Zwiesel, 615 m a.s.l., 3 km from the study site). Davi *et al.* (2011) found a difference in leafing of 8 days
20 between 2006 and 2007 for beeches in south-east France, however, in our study, where a single tree was observed, the difference was about 14 days.

The sigmoidal logistic fit after Richardson *et al.* (2007, 2009) seemed to neglect the pre and post leafing variations of the green%, which impacts little on year-to-year comparisons but leads to incorrect estimates of spring green-up if species
25 experience colour changes e.g. after leaf maturity. In our study a decreasing

amount of green after leaf unfolding caused a too early estimate of the start of the growing season.

Defining transition dates by calculating piecewise derivatives worked well for SOS which was estimated about 2 days before those from CPM. Ahrends *et al.* (2009)'s MAT dates, which were defined by the maximum green% value in a given time series, could describe end of leaf-up but in 2006 (see Fig. 3) they were incorrectly assigned to an outlier value derived from a cloudy day with an underexposed image. Ahrends *et al.* (2009) explained uncertainties of green% data amongst others by changing illumination conditions, so that camera observation requires "expert knowledge".

The CPM provides a reasonable autumn phenology analysis for foreground ROI. In the case of the aspen tree of ROI aspen2 the expected three change points, in both green% and red% data, matched perfectly. The other aspen tree of aspen1 did not show a strong leaf colouring and finally lost its (nearly almost green) leaves after the first snow falls. Therefore the CPM did not result in a three change point model as it did for beech and aspen2.

The results of Bayesian analysis for altitudinal bands were very encouraging, especially given the decreasing image quality due to increasing camera to tree distance as well as changing light and weather conditions. The CPM found expected change points at all observed altitudes in 2006 and 2007 and increasing uncertainties at greater distances and higher altitudes in 2006. By contrast, in 2007 the view on the Grosser Falkenstein mountain during leafing was clearer, and standard deviations in the higher altitude bands were smaller than at lower altitudes.

In both years the growing season at the lower altitude started 10 days earlier than the highest altitude i.e. a delay of about 2.5 days per 100 m. Similar results were

reported for 2006 and 2007 from south-east France (Davi *et al.* 2011) where a mean delay of leaf unfolding of 1.8 days per 100 m was observed on a slope from 961 to 1528 m. Guyon *et al.* (2011) detected a shift of about 1 day per 100 m in beeches on a slope of 100-1600 m in south-west France. Baumgartner (1962) investigated temperature gradients from the Grosser Falkenstein in 1955. In May he observed a mean temperature difference from 658 to 1157 m of 2.2 °C, from 796 to 1307 m of 4.2 °C, both about 500 m altitudinal difference. In his observation year he detected a shift of about one month (May 10 to June 8) in the appearance of the first leaf green of beech from 800 to 1200 m (Baumgartner *et al.* 1956). Dittmar & Elling (2006) analysed the altitudinal effect on leaf unfolding and leaf colouring of beech at 11 phenological stations (German Meteorological Service) distributed in the Bavarian Forest between 400-991 m from 1970 to 2000, excluding urban location and frost hollows, a delay of 2.3 days per 100 m was detected in leaf unfolding, and 0.8 days per 100 m in leaf colouring shift.

Our altitudinal analysis for autumn 2006 was less successful, since the CPM could not detect all expected change points and the transition dates for SEN, SOF and EOS did not show a clear pattern. This may have been caused by snowfalls close to the EOS date around DOY 300. After this date, the view on the slope of the Grosser Falkenstein was covered by clouds several times per week. Generally, detecting autumn colouring show more difficulties than observing leaf unfolding, since the phenological behaviour of individual trees varies more in autumn than in spring (Baumgartner 1952).

As for the spring analysis the previously published methods assessed in this study could not estimate precise transition days, nor their uncertainties during autumn leaf senescence.

The present study showed how Bayesian methods in the form of a multiple change point analysis could accurately describe phenological patterns derived from webcam photography. This was particularly true for spring green-up when the method successfully coped with high altitude phenology some considerable
5 distance from the camera. The results for autumn were less successful but for both seasons the Bayesian method showed considerably more credibility and reliability than established methods.

Acknowledgements

10 Financial support from the Bavarian State Ministry for Environment and Public Health is acknowledged. The authors thank the visitor centre of the Bavarian Forest National Park for providing the webcam data set. Raimund Henneken gratefully acknowledges the support by the Faculty Graduate Center Weihenstephan of TUM Graduate School at Technische Universität München,
15 Germany.

References

- Ahrends, H., Etzold, S., Kutsch, W., Stoeckli, R., Bruegger, R., Jeanneret, F., Wanner, H., Buchmann, N. & Eugster, W. (2009) Tree phenology and carbon dioxide fluxes: use of digital photography for process-based interpretation at the ecosystem scale. *Climate Research*, **39**, 261–274.
- Baumgartner, A. (1952) Zur Phänologie von Laubhölzern und ihre Anwendung bei lokalklimatischen Untersuchungen. *Berichte des Deutschen Wetterdienstes US-Zone*, **42**, 69-73.
- Baumgartner, A., Kleinlein, G. & Waldmann, G. (1956) Forstlich-phänologische Beobachtungen und Experimente am Großen Falkenstein (Bayerischer Wald). *Forstw Cbl*, **75**, 290–303.
- Baumgartner, A. (1962) Die Lufttemperatur als Standortfaktor am Gr. Falkenstein, 2. Mitteilung. *Forstwissenschaftliches Centralblatt*, **80**, 107-120.
- Davi H., Gillmann M., Ibanez T., Cailleret M., Bontemps A., Fady B. & Lefèvre F. (2011) Diversity of leaf unfolding dynamics among tree species: New insights from a study along an altitudinal gradient. *Agricultural and Forest Meteorology* (in press)
- Dittmar, C. & Elling, W. (2006) Phenological phases of common beech (*Fagus sylvatica* L.) and their dependence on region and altitude in Southern Germany. *Eur J Forest Res*, **125**, 181–188.
- Dose, V. & Menzel, A. (2004) Bayesian analysis of climate change impacts in phenology. *Global Change Biology*, **10**, 259–272.
- Garret, A.J.M. (1991) Ockham' s razor. *Maximum entropy and Bayesian methods* (eds W. Grandy & L. Schick). Kluwer Academics Publishers.
- Graham, E.A., Riordan, E.C., Yuen, E.M., Estrin, D. & Rundel, P.W. (2010) Public Internet-connected cameras used as a cross-continental ground-based plant phenology monitoring system. *Global Change Biology*, **16**, 3014–3023.
- Guyon, D., Guillot, M., Vitasse, Y., Cardot, H., Hagolle, O., Delzon, S. & Wigneron, J.-P. (2011) Monitoring elevation variations in leaf phenology of deciduous broadleaf forests from SPOT/VEGETATION time-series. *Remote Sensing of Environment*, **115**, 615–627.
- Ide, R. & Oguma, H. (2010) Use of digital cameras for phenological observations. *Ecological Informatics*, **5**, 339–347.
- Jacobs, N., Burgin, W., Fridrich, N., Abrams, A., Miskell, K., Braswell, B.H., Richardson, A.D. & Pless, R. (2009) The global network of outdoor webcams: properties and applications. *Proceedings of the 17th ACM SIGSPATIAL International Conference on Advances in Geographic Information Systems - GIS '09*, pp. 111–120. ACM Press.
- Jeong, S.-J., Ho, C.-H., Gim, H.-J. & Brown, M.E. (2011) Phenology shifts at start vs. end of growing season in temperate vegetation over the Northern Hemisphere for the period 1982-2008. *Global Change Biology*, **17**, 2385-2399.

- Kurc, S. & Benton, L. (2010) Digital image-derived greenness links deep soil moisture to carbon uptake in a creosotebush-dominated shrubland. *Journal of Arid Environments*, **74**, 585–594.
- 5 Menzel, A. (2002) Phenology: Its Importance to the Global Change Community GLOBAL CHANGE COMMUNITY. *Climatic Change*, **54**, 379–385.
- Menzel, A. (2003) Plant phenological anomalies in Germany and their relation to air temperature and NAO. *Climatic Change*, **57**, 243–263.
- 10 Menzel, A., Sparks, T.H., Estrella, N., Koch, E., Aasa, A., Ahas, R., Alm-Kübler, K., Bissolli, P., Braslavská, O., Briede, A., Chmielewski, F.M., Crepinsek, Z., Curnel, Y., Dahl, Å., Defila, C., Donnelly, A., Filella, Y., Jateczak, K., Máge, F., Mestre, A., Nordli, Ø., Peñuelas, J., Pirinen, P., Remišová, V., Scheifinger, H., Striz, M., Susnik, A., van Vliet, A.J.H., Wielgolaski, F.-E., Zach, S. & Zust, A.N.A. (2006) European phenological response to climate change matches the warming pattern. *Global Change Biol*, **12**, 1969–1976.
- 15 Menzel, A., Estrella, N., Heitland, W., Susnik, A., Schleip, C. & Dose, V. (2008) Bayesian analysis of the species-specific lengthening of the growing season in two European countries and the influence of an insect pest. *Int J Biometeorol*, **52**, 209–218.
- 20 Nagai, S., Maeda, T., Gamo, M., Muraoka, H., Suzuki, R. & Nasahara, K.N. (2011) Using digital camera images to detect canopy condition of deciduous broad-leaved trees. *Plant Ecology & Diversity*, **4**, 79–89.
- Richardson, A.D., Jenkins, J.P., Braswell, B.H., Hollinger, D.Y., Ollinger, S.V. & Smith, M.L. (2007) Use of digital webcam images to track spring green-up in a deciduous broadleaf forest. *Oecologia*, **152**, 323–334.
- 25 Richardson, A.D., Braswell, B.H., Hollinger, D.Y., Jenkins, J.P. & Ollinger, S.V. (2009) Near-surface remote sensing of spatial and temporal variation in canopy phenology. *Ecological Applications*, **19**, 1417–1428.
- 30 Rosenzweig, C., Karoly, D., Vicarelli, M., Neofotis, P., Wu, Q., Casassa, G., Menzel, A., Root, T.L., Estrella, N., Seguin, B., Tryjanowski, P., Liu, C., Rawlins, S. & Imeson, A. (2008) Attributing physical and biological impacts to anthropogenic climate change. *Nature*, **453**, 353–357.
- Schleip, C., Menzel, A., Estrella, N. & Dose, V. (2006) The use of Bayesian analysis to detect recent changes in phenological events throughout the year. *Agricultural and Forest Meteorology*, **141**, 179–191.
- 35 Schwartz, M.D. (2003) Phenology. An integrative environmental science. Kluwer Acad. Publ, Dordrecht.
- Sparks, T.H., Menzel, A. & Stenseth, N.C. (2009) European cooperation in plant phenology. *Clim. Res*, **39**, 175–177.
- 40 Zhang, X.Y., Friedl, M.A., Schaaf, C.B., Strahler, A.H., Hodges, J.C.F., Gao, F., Reed, B.C. & Huete, A. (2003) Monitoring vegetation phenology using MODIS. *Remote Sensing of Environment*, **84**, 471–475.

Tables

Table 1: Transition date analysis of ROI in spring 2006 and 2007 based on green% data. CPM analysis: RSMD = the root mean square deviation, nCP = number of change points in the best model fit, SD = standard deviation, DIF = 5 MAT-SOS. Compared methods: SOS and MAT dates (Ahrends *et al.* 2009), hspring date based on the sigmoidal logistic fit (Richardson *et al.* (2007)).

	ROI	fits of CPM		results of CPM					compared methods			
		RMSD	nCP	SOS	SD	MAT	SD	DIF	SOS	MAT	DIF	hspring
2006	beech	0.0076	2	125	0.4	135	0.3	10	125	138	13	130
	aspen1	0.0077	2	128	0.5	137	0.6	10	126	150	24	131
	aspen2	0.0074	2	124	2.1	151	1.4	27	132	150	18	134
2007	beech	0.0089	2	111	0.6	123	1.1	12	112	129	17	116
	aspen1	0.0122	2	116	1.7	125	1.7	8	114	129	15	118
	aspen2	0.0119	2	130	1.3	135	1.3	6	125	138	13	131

Table 2: Transition date analysis of ROI in autumn 2006 based on green% and red% data. CPM analysis: RSMD = the root mean square deviation, nCP = number of change points in the best model fit, SD = standard deviation. For the beech and aspen2 ROI of green% time series, SEN, SOF and EOS were estimated from the first, third and fourth change points respectively. Compared methods: SEN and EOS dates (Ahrends *et al.* 2009), hautumn and xautumn dates based on the sigmoidal logistic fit (Richardson *et al.* (2007, 2009).

ROI		fits of CPM		results of CPM						compared methods			
		RMSD	nCP	SEN	SD	SOF	SD	EOS	SD	SEN	EOS	hautumn	xautumn
beech	green%	0.0057	4	241	2.6	292	0.5	301	6.2	242	293	268	
	red%	0.0278	3	244	12.7	288	3.3	307	6.8				286
aspen1	green%	0.0078	2	304	1.5			309	1.8	292	313	308	
	red%	0.0294	1			305	5.9						304
aspen2	green%	0.0066	4	290	2.2	301	0.3	305	2.8	275	304	293	
	red%	0.0293	3	288	2.6	302	1.0	307	0.6				300

Table 3: Change points in 100m altitudinal bands (700-1200 m) in spring 2006 and 2007 based on green% data. SD = standard deviation, DIF = MAT-SOS, RSMD = the root mean square deviation, nCP = number of change points in the best model fit. For the 800-900 m band in 2006, SOS and MAT were interpreted as the first and second change point respectively.

	Altitudinal band	SOS	SD	MAT	SD	DIF	RMSD	nCP
2006	1100-1200	130	2.6	137	4.8	8	0.0035	2
	1000-1100	125	3.3	134	3.6	9	0.0032	2
	900-1000	124	2.2	130	2.1	5	0.0034	2
	800-900	123	2.2	130	1.2	7	0.0030	3
	700-800	120	1.9	129	1.2	9	0.0048	2
2007	1100-1200	112	1.0	120	0.8	8	0.0033	2
	1000-1100	111	1.4	119	1.7	8	0.0030	2
	900-1000	106	2.8	117	2.1	11	0.0034	2
	800-900	103	2.5	115	2.2	12	0.0038	2
	700-800	102	1.9	114	2.2	12	0.0056	2

Table 4: Change points in altitudinal bands in autumn 2006 based on green% and red% data. SD = standard deviation, RSMD = the root mean square deviation, nCP = number of change points in the best model fit.

altitudinal band		SEN	SD	SOF	SD	EOS	SD	RMSD	nCP
1100-1200	green%	281	3.4	290	2.4	299	2.9	0.0025	3
	red%			330	23.1			0.0145	1
1000-1100	green%	272	9.5	291	5.1	302	8.4	0.0023	3
	red%			334	28.7			0.0138	1
900-1000	green%	265	14.9			292	16.6	0.0027	2
	red%			330	15.6			0.0135	1
800-900	green%	268	8.5			291	6.8	0.0028	2
	red%			319	16.0			0.0145	1
700-800	green%	281	4.4			296	2.5	0.0040	2
	red%			299	6.8			0.0168	1

Figures

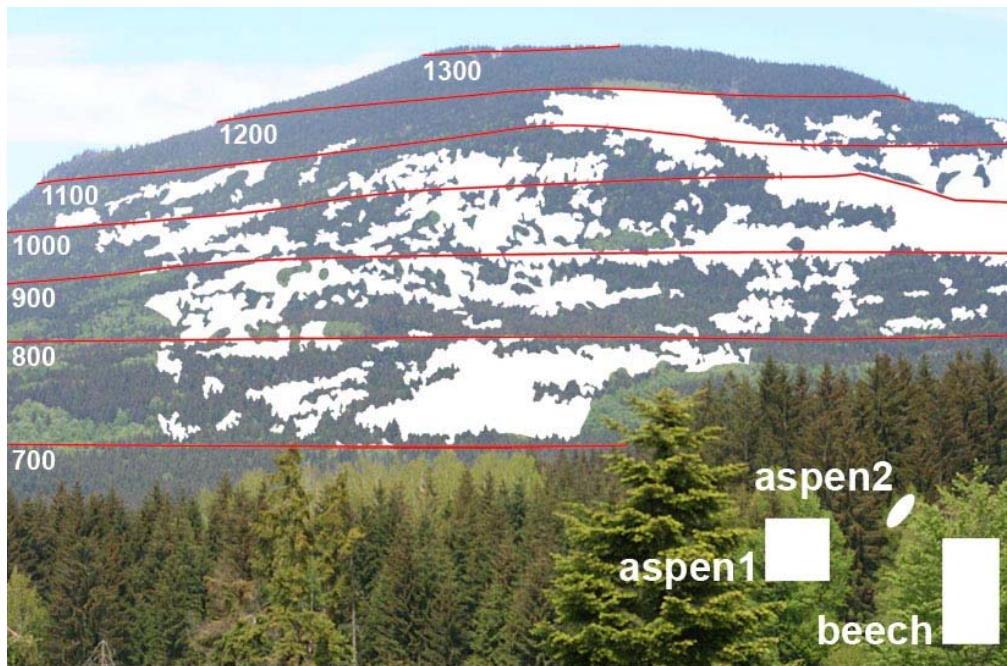


Fig. 1: Sample image of the “Großer Falkenstein“ (recorded May 22 2006, DOY 142). White sections indicate regions of interest (ROI), contours from 700 to 1300 m in 100 m steps are shown in red. ROI: Aspen1 and aspen2: Common Aspen, beech: Common Beech, non-numbered sections on the slope refer to altitudinal ROI (700-1200 m). The left hand part of the image was excluded from the analysis because it wasn't visible during the whole time series due to interference from a foreground tree close to the camera.

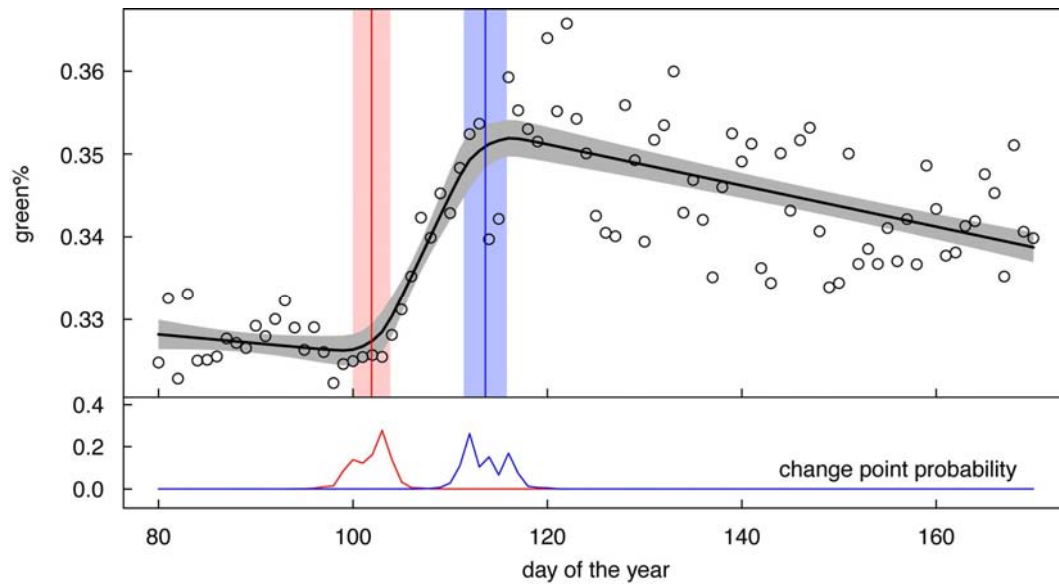


Fig. 2: Multiple change point representation of green% data in spring shown as open circles. The heavy continuous curve is the expectation value, the shaded band the $\pm 1\sigma$ uncertainty of this estimate. The lower panel shows the normalised change point probability distributions. A summary of these distributions in terms of mean and $\pm 1\sigma$ uncertainty is shown by the vertical lines with shaded bands.

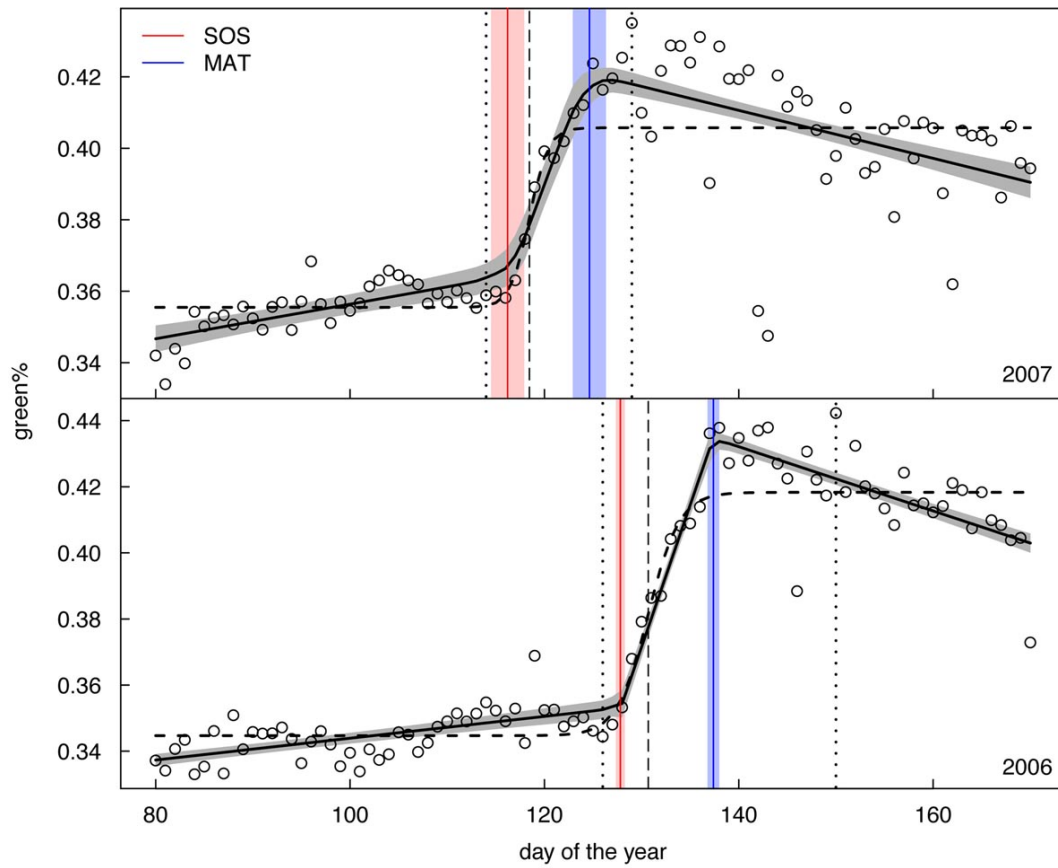


Fig. 3: Bayesian change point models of green% of aspen1 in spring 2006 and 2007. For a general description see Fig. 2. Dashed vertical line shows hspring value based on the sigmoidal logistic fit (Richardson *et al.* (2007), dashed line),
 5 dotted lines show SOS and MAT dates (Ahrends *et al.* 2009). Parameters of the Bayesian model fit are given in Table 1.

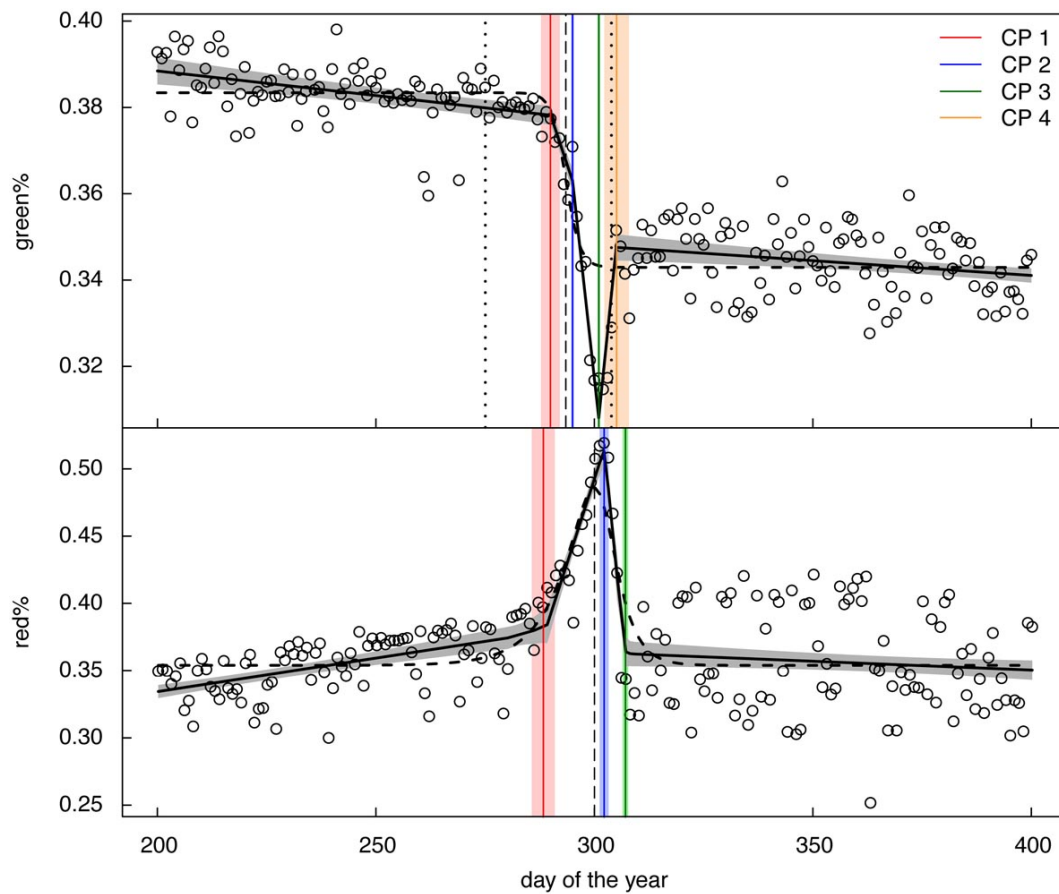


Fig. 4: Bayesian change point models of green% and red% of aspen2 in autumn 2006. For a general description see Fig. 2. Dashed vertical lines show hautumn and xautumn values based on the sigmoidal logistic fit (Richardson *et al.* (2007, 5 2009), dashed line), dotted lines show SEN and EOS dates (Ahrends *et al.* 2009). Parameters of the Bayesian model fit are given in Table 2.

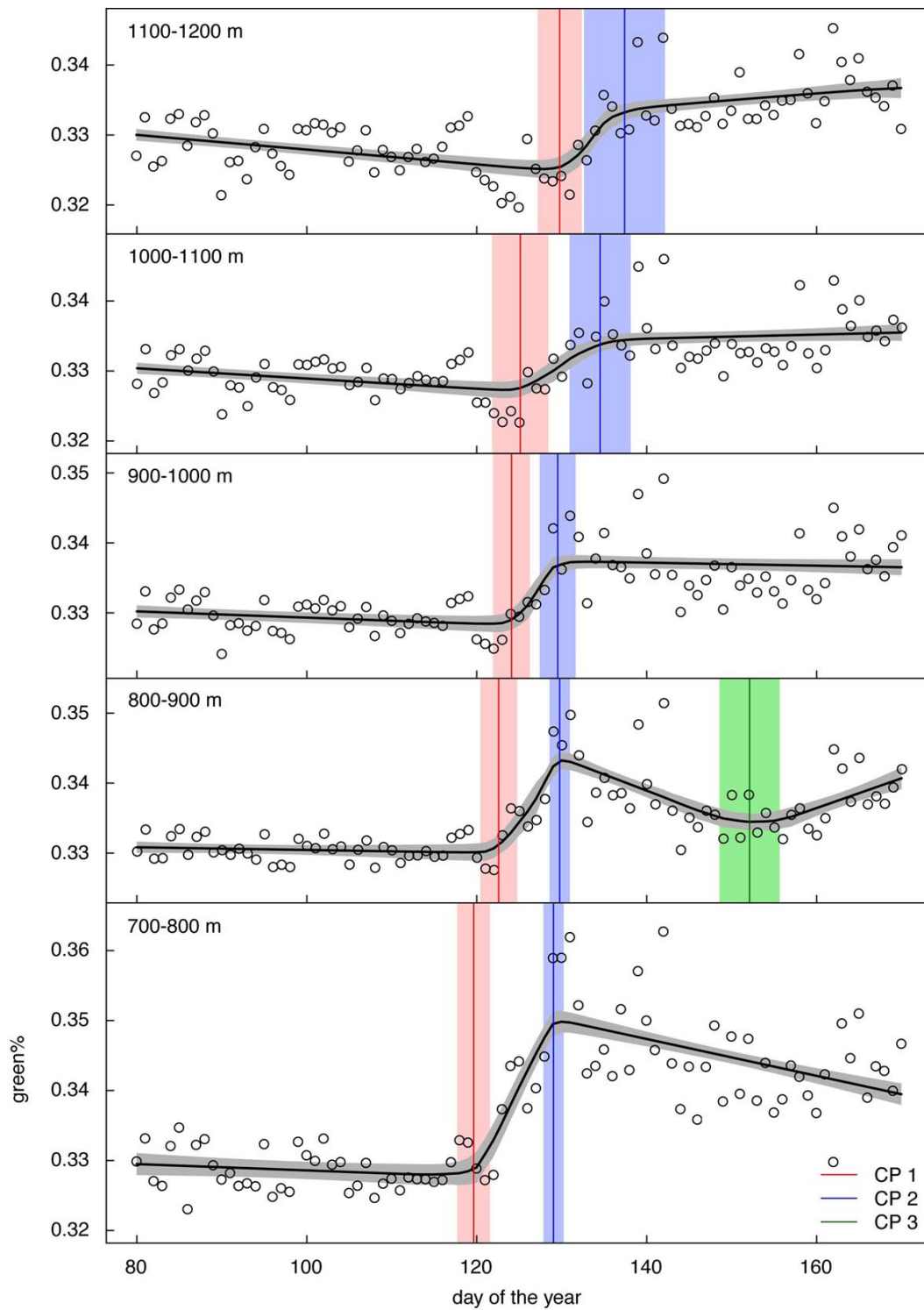


Fig. 5: Bayesian change point models of green% in 100m altitudinal bands (700-1200 m), spring 2006. For a description see Fig. 2. Parameters of the Bayesian model fit are given in Table 3.